MULTI-SCALE AND MULTI-PHYSICS COUPLED MODELING OF THE EVOLUTION OF INTERNAL STRESSES AND PART SHAPE OF CARBON-EPOXY COMPOSITES

M. Hirsekorn[1*], G. Grail[1], M. Poitrimolt[1], R. Agogué[1], P. Beauchêne[1]

[1]*Onera – The French Aerospace Lab, 29 avenue de la Division Leclerc, F-92322 Châtillon, France*
**e-mail address of the corresponding author: martin.hirsekorn@onera.fr*

Keywords: cure kinetics, internal stresses, multi-scale, coupled modeling

Abstract
A multi-scale modeling strategy is presented that couples the different physics contributing to the generation of internal stresses in carbon-epoxy composites: Cure reaction kinetics, heat transfer, mechanical behavior of the constituents, and the coupling between them are modeled simultaneously over the whole curing process, including the heating, curing, and cooling stages. The method is applied to the case of an asymmetric [0/90] laminate made of a T700/M21 prepreg lay-up, cured under pressure in a closed mold. The predicted final shape is in good agreement with the experimental observations. Thermal and mechanical boundary conditions influence significantly the internal stresses and hence the warpage of the laminate.

1 Introduction

The good ratio between mechanical performances and weight, together with improving design and modeling tools allowing for a better estimation of strength and lifetime, brings the aerospace industry to increasingly use composite materials in primary structures and geometrically complex parts. This provokes on the one hand an increasing need of thicker parts capable of carrying higher loads, and on the other hand of complex shapes with curved sections, varying thickness or branching. Both features potentially intensify the effects of residual stresses, which are ubiquitous in organic matrix composites, because of the high contrast between the mechanical properties of the polymer matrix and the reinforcing fibers, and because most polymers used in composite materials have to be cured at temperatures much higher than the service temperature.

The effects of residual stresses have been summarized by Parlevliet et al. [1]: They influence strength [2], since they add up to external forces, in most cases reducing compressive strength, while tensile strength may increase for certain load cases. They may cause defects such as increased fiber waviness, matrix damage or fiber-matrix decohesion – under some circumstances even early in the cure cycle, because triaxial tensile stress states may damage the matrix shortly after gelation, when it is still weak [3], even though shear stresses are quickly relaxed. At the structure level, imbalanced residual stresses cause part distortions, particular important in asymmetric lay-ups. However, warpage may even occur if the reinforcement architecture is symmetric [4], because of tool-part interaction. Curved sections usually undergo spring-in – a reduction of the curvature radius due to cure shrinkage and thermal contraction of the matrix [5]-[6]. In industrial design of composite structures, these issues are most often tackled by a trial-and-error strategy. An accurate modeling tool, able to

predict the effects of residual stresses and the final shape of a composite part would therefore greatly reduce the production costs of complex composite structures.
Residual stresses and part distortions are often simulated using a simple thermoelastic approach that accounts for the thermal contraction of fibers and matrix during post-cure cooling. This may be sufficient in asymmetric [0/90] laminates, where 95% of the part distortion is due to thermoelastic effects [3]. However, in curved parts, such as L-angles, only about 50% of the total spring-in is due to thermoelastic effects [5], the other 50% being mostly due to chemical shrinkage during the cure cycle. In fact, internal stresses also develop during the hot stage of curing [7], when the resin first expands due to heating and then shrinks chemically. The coupling between the exothermal cure reaction and its thermal activation is particularly pronounced in thick composite parts, in which significant overheating may occur [8], potentially causing resin degradation. Such thermal inhomogeneities also cause considerable gradients of cure and thus of matrix properties, which contribute to the residual stress formation and may even cause matrix damage. Finally, bending moments may be built up during the heating phase before curing, due to tool-part interaction [9]. These moments are "frozen" into the resin while it cures and cause part distortion after demolding.
The formation of residual stresses in composite materials is thus a multi-physics coupled problem including the cure kinetics of the polymer matrix, heat transfer within the part and between the molding tool and the part, and mechanical interaction between matrix, reinforcement and molding tool. The coupling is particularly important in thick composite parts and in complex structures with curved parts, varying thickness, or imbalanced fiber architecture. Furthermore, composites are intrinsically multi-scale, and residual stresses have significant effects at all scales, reaching from the micro-scale of a single fiber up to the scale of the whole structure. In this contribution, we present a multi-scale and multi-physics coupled modeling strategy to predict residual stresses and the final shape of composite parts. The objective is to model the whole curing cycle, including heating, curing, and cooling phases, in order to take into account all effects that contribute to the formation of residual stresses and the coupling between them. In Section 2 we present the coupling between cure kinetics and heat transfer modeling. The coupling between thermo-kinetic and thermo-mechanic modeling is presented in Section 3. In Section 4, we give a short overview on the multi-scale modeling strategy. Finally, an application is shown in Section 5.

2 Coupled modeling of cure kinetics and heat transfer

In most long fiber reinforced polymer composites, the fiber volume fraction is relatively high (above 50%). Therefore, once the resin injection has finished and the curing cycle starts, convection becomes negligible [10]. This may not be true in the case of pure resin, but since we focus on the curing of composites, we can assume that heat transfer occurs only due to conduction. Likewise, the evolution of the degree of cure depends only on the local temperature. The heat generated by the exothermal cure reaction can thus be included into the heat transfer equation by the addition of a source term [10], which only depends on local variables. The reaction heat is proportional to the cure rate, and the proportionality factor is the total reaction enthalpy H_R:

$$\nabla \cdot \left(\underline{\underline{\kappa}}(c,T) \nabla T \right) = \rho \left(-C_p(c,T) \frac{dT}{dt} + H_R \frac{dc}{dt} \right) \tag{1}$$

$\underline{\underline{\kappa}}$ is the homogenized thermal conductivity tensor of the matrix-reinforcement ensemble (see Section 4). ρ is its average mass density and C_p the average specific heat. Cure kinetics of thermosetting resins is frequently simulated using the autocatalytic model of Kamal and Sourour [11]. A modified version has been proposed by Karkanas et al. [12]:

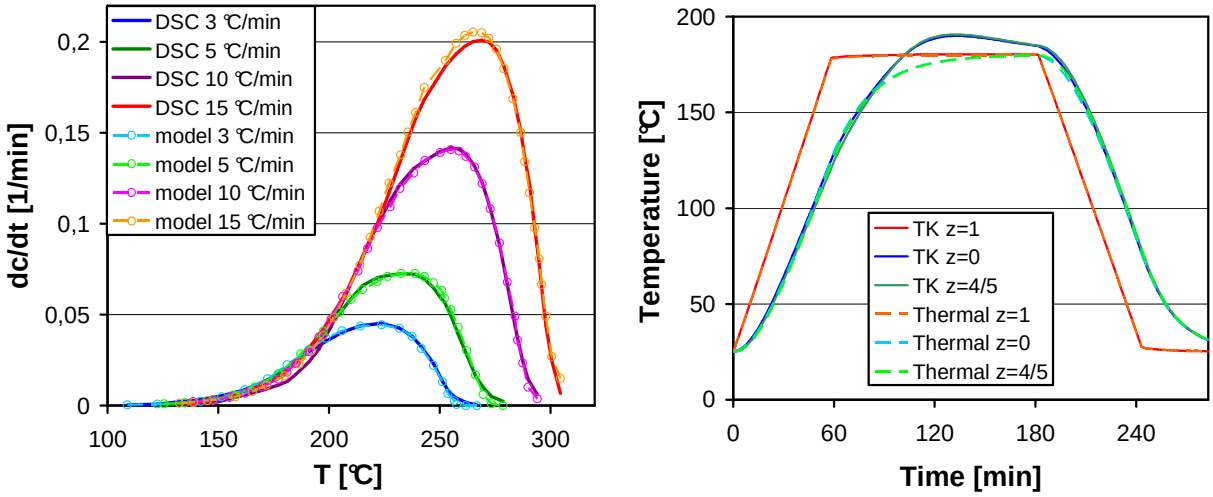

Figure 1. Left : Identification of cure kinetics model of the resin M21 based upon DSC data by Msallem [13]. Right : Temperature evolution at different vertical positions (z = fraction of total thickness) at the center of a T700/M21 composite throughout the cure cycle obtained by purely thermal and coupled thermokinetic (TK) modeling.

$$\frac{dc}{dt} = A_1 \exp\left(-\frac{E_1}{RT}\right)(1-c)^{n_1} + A_2 \exp\left(-\frac{E_2}{RT}\right)c^m(1-c)^{n_2} \qquad (2)$$

with A_i being reaction rate constants, E_i activation energies, R the ideal gas constant, and m and n_i reaction orders. This modified model has been found to better fit the cure kinetics of the M21 epoxy resin measured by means of dynamic DSC (Differential Scanning Calorimetry) by Msallem [13] (see Figure 1).

Eq. 1 is solved using Finite Elements (FE) in the same way as a standard conductive heat transfer problem. The right side of Eq. 1 has to be integrated locally over the time step. In a standard heat transfer problem, this is done only for the term containing the specific heat, yielding the heat that is absorbed or released by the material due to its temperature change. In the coupled problem, the reaction enthalpy released over the time step is added. Since the cure kinetics Eq. 2 can be solved locally, the degree of cure is treated as an internal variable of the thermal behavior of the composite material. Its evolution over the time step is calculated using the backward Euler method with Newton-Raphson iteration locally at each integration point, taking into account the local temperature evolution.

As an example of a coupled thermo-kinetic simulation we model the curing of a square plate made of T700/M21 prepreg in an autoclave. The plate thickness is 1.5cm, the side length 20cm. We impose convective heat transfer at the boundaries, with a heat transfer coefficient of 10.5 kW/(m^2·K), corresponding to 1cm of Invar, at the bottom side, and 0.01 kW/(m^2·K), corresponding to dry air, at the remaining boundaries. Specific heat and heat conductivity both depend on temperature and cure. The values measured by Msallem [13] are used for the M21 resin, and the composite properties are obtained by homogenization as described in Section 4, with a fiber volume fraction of 60%. The results are compared to a heat transfer simulation without cure kinetics, using the properties of the cured resin. Figure 1 shows that the bottom side follows well the imposed temperature cycle, while the top side lacks behind, due to the low heat transfer coefficient at the top boundary. After the onset of polymerization, the material is additionally heated by the exothermal cure reaction. The reaction heat is conducted away rapidly at the bottom side, but leads to significant overheating in the upper half plate. The maximum temperature is reached at 4/5 of the plate thickness. Due to the good conductivity of the fibrous reinforcement, the overheating remains acceptable, and leads to a quite homogeneous final degree of cure, compensating the delayed heating of upper half plate.

3 Coupling of thermokinetic to thermomechanic modeling

The coupling between thermokinetic and thermomechanic modeling is due to the dependence of the material behavior on temperature and degree of cure. Furthermore, thermal dilatation and chemical shrinkage have to be taken into account. Since strain rates are low during the curing process, there will be no heat generation due to plastic dissipation. In addition, we assume that the cure kinetics and the thermal properties are independent of pressure or shear stress. The thermokinetics is thus not influenced by the mechanics, and it is possible to carry out two sequential FE calculations: First the coupled thermokinetic simulation described in the previous section, which yields for each integration point the local evolution of temperature and degree of cure with time, and then a mechanical FE simulation, which uses these data as local parameters to the material behavior. Two parametric strains are added to the constitutive model, such that the total material strain is given by

$$\underline{\varepsilon} = \underline{\varepsilon}_{mech} + \underline{\varepsilon}_{th} + \underline{\varepsilon}_{ch} \tag{3}$$

The increments of thermal strain $\underline{\varepsilon}_{th}$ and the chemical strain $\underline{\varepsilon}_{ch}$ are calculated by integration over the time step of

$$\frac{d\underline{\varepsilon}_{th}}{dt} = \underline{\alpha}_{th}(c,T)\cdot\frac{dT}{dt} \text{ and } \frac{d\underline{\varepsilon}_{ch}}{dt} = \underline{\alpha}_{ch}(c,T)\cdot\frac{dc}{dt} \tag{4}$$

where $\underline{\alpha}_{th}$ is the tensor of thermal expansion and $\underline{\alpha}_{ch}$ the tensor of chemical shrinkage. In the mechanical constitutive model, these two strains are subtracted from the total strain, and stress is calculated as a function of the mechanical strain $\underline{\varepsilon}_{mech}$ only.

A purely elastic constitutive model causes an overestimation of the residual stresses of as much as 20% [14], because stress relaxation effects are not taken into account. The mechanical behavior of the resin is therefore modeled using a linear viscoelastic generalized Maxwell model [15]. With this model, the relaxation modulus (stress response under constant strain divided by this strain) is represented by a Prony series:

$$\mathbf{E}(t) = \mathbf{E}_{\infty} + \sum_{i=1}^{N} \omega_i \exp\left(-\frac{t-t_0}{\tau_i}\right)\left(\mathbf{E}_0 - \mathbf{E}_{\infty}\right) \tag{5}$$

in which each term corresponds to one Maxwell element. $\mathbf{E}_0$ is the instantaneous and $\mathbf{E}_{\infty}$ the relaxed modulus. In general, one relaxation time τ_i per decade is sufficient to describe the relaxation curves of polymers [16]. The weights ω_i have been identified by fitting Eq. 5 to the relaxation master curve for in-plane shear of a fully cured T700/M21 unidirectional (UD) composite at a reference temperature of 198°C (Figure 2). In the construction of the master curve, a thermo-rheologically simple behavior [15] has been assumed, i.e., the temperature only changes the relaxation times, while weights and instantaneous and relaxed moduli are independent of temperature. In this case, a change of temperature corresponds to a shift of the relaxation curve along the logarithmic time scale by a temperature dependent shift factor.

The influence of the degree of cure on the matrix behavior is modeled assuming a thermo-chemo-rheologically simple behavior [6][14]. In this case, the shift factor is assumed to depend only on the difference between material temperature and the current glass transition temperature T_g. The relaxation times are hence given by

$$\tau_i(T, c) = \tau_i(T_{ref}) \cdot 10^{-1.88 - 0.112/\mathrm{K}\cdot\left(T - T_g(c)\right)} \tag{6}$$

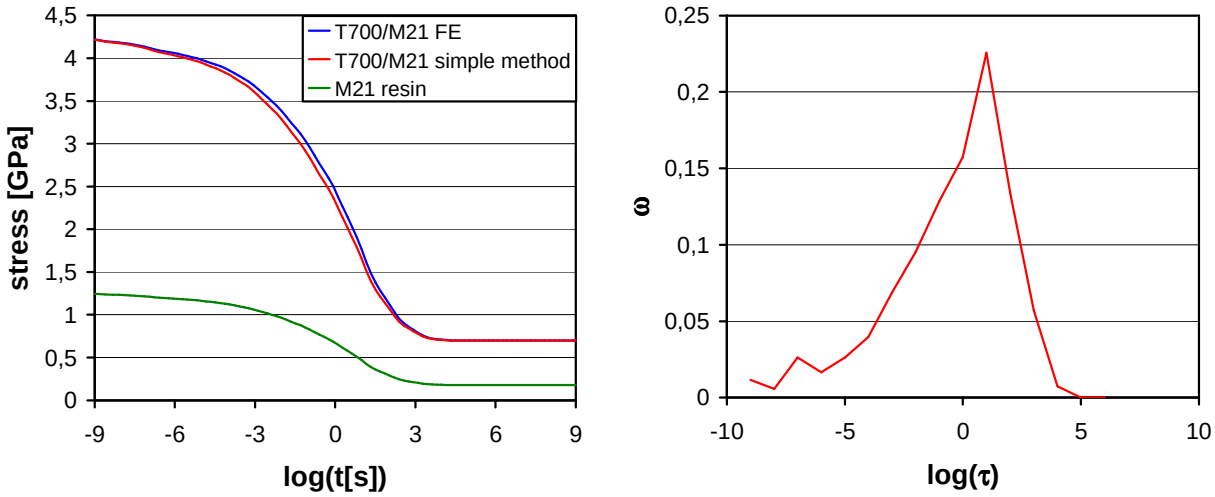

Figure 2. Left : In-plane shear relaxation curves at the reference temperature of 198°C of the pure M21 resin and of the T700/M21 composite obtained by two different homogenization methods. Right : Relaxation time spectrum obtained from the in-plane shear relaxation master curve of a T700/M21 UD composite plate.

The coefficients of Eq. 6 are obtained by determining the shift along the logarithmic time axis necessary to superpose the relaxation curves observed at different temperatures to a single master curve at the reference temperature. The glass transition temperature as a function of the degree of cure follows DiBenedetto's equation, and the coefficients have been determined by Msallem [13] for the M21 resin.

4 Multi-scale modeling and homogenization

In general composite structures have (at least) three characteristic scales: The *micro-scale* at which single fibers are treated separately, the *meso-scale* of a yarn in a composite with woven reinforcements or of a ply in a laminate, and the *macro-scale* of the whole structure. Therefore, a multi-scale modeling strategy has to be adopted, which is usually based upon homogenization and localization techniques. The principle is to define a representative volume element (RVE) of the smaller scale, compute the homogenized properties of this RVE and to use these properties to model the next higher scale. This can be done using a FE representation of the RVE with appropriate boundary conditions. In the example shown in Section 5, each ply of the laminate is explicitly taken into account in the macro-scale simulation. However, homogenization at the micro-scale is necessary in order to derive the ply properties and their evolution with temperature and degree of cure from the properties of the fibers and the matrix. At the micro-scale, a long-fiber reinforced composite is best described by a random fiber distribution of at least 10 parallel fibers [17] with periodic boundary conditions. However, if only linear properties have to be homogenized, a hexagonal RVE containing a single fiber is sufficient.

The homogenized elastic stiffness tensor can be obtained by applying consecutively the 6 elementary strains (only one component of the strain tensor is not zero) as an average strain to the RVE. The resulting average stresses correspond to the respective columns of the stiffness tensor in Voigt notation (6x6 matrix). In order to obtain the homogenized viscoelastic behavior of a composite ply, we use a simplified method: We assume that the relaxation spectrum of the composite under any kind of load is the same and equal to that of the matrix. Then, it is sufficient to homogenize the instantaneous and the relaxed stiffness tensor applying the same method as for the homogenization of an elastic material. This is necessary, because we know the full relaxation master curve only under in-plane shear, and in transverse and fiber direction only the instantaneous elastic properties of the UD ply.

The time and temperature dependence of the bulk modulus of a polymer is very weak, while there is significant relaxation and temperature dependence in tension and shear [18]. We can therefore assume that the instantaneous and the relaxed stiffness tensor of the isotropic matrix only differ in the shear component. These components can be derived from the asymptotic values of the in-plane shear relaxation curve of the UD ply by inverse identification. The resulting shear relaxation modulus of the matrix, obtained using the same spectrum as for the in-plane shear relaxation of the composite, is shown in Figure 2. Using the longitudinal fiber modulus provided by the manufacturer and the transverse fiber modulus and Poisson ratios obtained by inverse identification on the instantaneous elastic properties of the UD ply, the relaxation curves of the UD ply under any kind of load can be obtained either by FE homogenization or using the simplified method. In Figure 2 both methods are compared. It can be seen that the simplified method yields a slightly faster relaxation than the FE method. The difference between both methods is comparable for transverse tension and out-of-plane shear, but much smaller for the fiber dominated longitudinal tension.
The thermal conductivity can be homogenized in the same way as the elastic stiffness, by simply replacing the elementary strains by temperature gradients in the same directions and taking the resulting stress components as the vector of heat flow. The coefficients of thermal expansion and chemical shrinkage are homogenized by applying a homogeneous temperature or degree of cure change to the whole RVE and dividing the resulting strain by the applied ΔT or Δc. Scalar properties, such as mass density, specific heat, and reaction enthalpy are homogenized by a simple rule of mixture, taking zero reaction enthalpy for the fibers. The required properties of fibers and matrix are taken from Msallem [13]. The reaction kinetics only applies to the matrix, and is thus the same for the composite (the only difference is the reaction enthalpy).

5 Prediction of internal stresses and final part shape

The presented approach has been used to model the curing process of an asymmetric $[0_4/90_4]$ laminate made of T700/M21 prepreg by Hexcel. The curing cycle follows the temperature curve shown by the red line in Figure 1. However, contrary to the case presented there, the plate is in contact with the stainless steel mold at the bottom as well as at the top side. Both sides are heated. Furthermore, the final plate thickness is only 2mm, such that there are no significant temperature gradients during the cure cycle. When the mold reaches the curing temperature of 180°C, a pressure of 7bar is applied by a hydraulic press. The curing temperature is held for 2 hours. Then the mold is cooled down to room temperature. The pressure is released at the end of the cooling. After demolding, the laminate immediately jumps to the shape shown in Figure 3. The vertical displacement of the center of the long edge with respect to the plate corners is 19.8mm, which corresponds to a curvature radius of 550mm, that of the short edge it is 2.3mm, which corresponds to a curvature radius of 1190mm. Since the lay-up is perfectly antisymmetric, the same curvature radius in both directions would be expected. The difference is probably due to mechanical interaction between the mold and the prepregs during the cure cycle.
Thermokinetic and thermomechanic modeling of the whole cure cycle using the viscoelastic model described above yield a significant flexion of the plate during the initial heating phase in opposite direction to the flexion that occurs during the cooling phase. However, since the resin is totally uncured during the heating stage, any significant stress leading to plate flexion should be immediately relaxed. This is not the case with the relatively high relaxed matrix shear modulus identified from Figure 2, which is about 14% of the instantaneous modulus.
Since in the fully cured state at temperatures significantly below T_g (215°C for $c = 1$) total stress relaxation is never reached, the relaxation modulus has a negligible impact on the cooling phase. However, it significantly influences stress relaxation during the cure cycle.

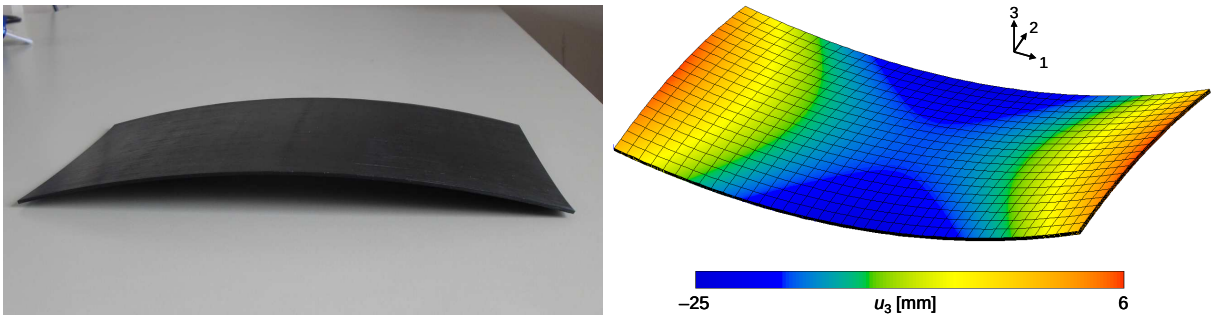

Figure 3. Left : T700/M21 [0_4/90_4] plate after demolding. Right : Vertical displacement map obtained from the coupled multi-scale modeling of the curing process.

Since before gelation, shear stresses should be fully relaxed, a much smaller relaxed shear modulus (e.g., 1% of the instantaneous modulus) seems more reasonable. This is the same order of magnitude as the ratio between rubbery and glassy modulus of typical epoxy resins (e.g., [6][15]). Using this reduced relaxed modulus in the coupled modeling, the plate warps only slightly during heating and during the curing cycle. The final edge displacements with respect to the corners are 21.5mm for the long side and 5.4mm for the short side, both corresponding to a curvature radius of 505mm.
The influence of the mold is modeled by imposing flat bottom and top sides and applying the mold pressure to the top side. These conditions are released gradually at the end of the cooling cycle, in order to avoid numerical instabilities. Due to these boundary conditions additional stresses appear within the laminate, which influence relaxation and the final stress state at the end of the cooling cycle. The edge displacements after releasing the boundary constraints are 20.8mm at the long side and 4.8mm at the short side, corresponding to curvature radii of 522mm and 571mm, respectively. The flexion in the direction of the long side of the plate is quite close to that observed experimentally. However, there is still a significant discrepancy from the observed flexion in direction of the short side. Applying mold constraints during cure modeling provokes an asymmetry in the flexion, but the effect is much smaller than observed in the experiment. However, this result indicates that tool-part interaction may be at the origin of the difference in curvature radii, and must be taken into account in the coupled modeling of the curing process.

6 Conclusions

The presented multi-scale and multi-physics approach can be applied to the modeling of the entire curing process of thermosetting matrix composites, including heating, curing, and cooling phase. It takes into account the mutual coupling between cure reaction kinetics, heat transfer, and mechanical behavior at the different characteristic scales of the composite part. Thermal and mechanical boundary conditions are taken into account, and the interaction between tool and composite part can be easily integrated into the modeling process. The method has been applied to the case of an asymmetric laminate. The final shape predicted by the modeling tool is in good agreement with the real test specimen. The example has shown that the interaction between tool and part is not negligible, and must therefore be taken into account in the boundary conditions, or modeled explicitly by including the tool in the modeling setup. The influence of sliding between plies and tangential friction between the part and the mold has not yet been considered, but will be included in future simulations. Further ongoing work focuses on in-situ measuring of residual strains using optical fibers with Bragg gratings, in order to validate the model predictions at a more local level. Finally, a natural difficulty in multi-scale and multi-physics coupled modeling is the large number of material properties that have to be identified experimentally. For example, the polymer matrix

has to be characterized at different temperatures and degrees of cure, covering the ranges occurring in the curing cycle.

References

[1] Parlevliet P.P., Bersee H.E.N., Beukers A. Residual stresses in thermoplastic composites – a study of the literature. Part III: Effects of thermal residual stresses. *Composites Part A* **38,** 1581-1596 (2007).

[2] Fiedler B., Hojo A., Ochiai S. The influence of thermal residual stresses on the transverse strength of CFRP using FEM. *Composites Part A* **33,** 1323-1326 (2002).

[3] Wisnom M.R., Gigliotti M., Ersoy N., Campbell M., Potter K.D. Mechanisms generating residual stresses and distortion during manufacture of polymer-matrix composite structures. *Composites Part A* **37,** 522-529 (2006).

[4] Twigg G., Poursartip A., Fernlund G. Tool-part interaction in composites processing. Part I: experimental investigation and analytical model. *Composites Part A* **35,** 121-133 (2004).

[5] Ersoy N., Potter K., Wisnom M.R., Clegg M.J. Development of spring-in angle during cure of a thermosetting composite. *Compososites Part A* **36,** 1700-1706 (2005).

[6] Svanberg J.M., Holmberg J.A. Prediction of shape distortions. Part II. Experimental validation and analysis of boundary conditions. *Composites Part A* **35,** 723-734 (2004).

[7] Rabearison N., Jochum C., Grandidier J.C. A FEM coupling model for properties prediction during the curing of an epoxy matrix. *Comput Mater Sci* **45,** 715-724 (2009).

[8] Balvers J.M., Bersee H.E.N., Beukers A. *Determination of cure dependent properties for curing simulation of thick-walled composites* in Proceedings of *the 49th AIAA/ASME/ASCE/AHS/ASC Structures, Structural Dynamics, and Materials Conference*, Schaumburg, IL (2008).

[9] Twigg G., Poursartip G., Fernlund G. Tool-part interaction in composites processing. Part II: numerical modelling. *Composites Part A* **35,** 135-141 (2004).

[10] Skordos A.A., Partridge I.K. *Monitoring and heat transfer modelling of the cure of thermoset composites processed by resin transfer moulding (RTM)* in Proceedings of *Polymer Composites '99*, Québec, Canada (1999).

[11] Kamal M.R., Sourour S. Differential scanning calorimetry of epoxy cure: Isothermal cure kinetics. *Thermochim Acta* **14,** 41-59 (1976).

[12] Karkanas P.I., Partridge I.K., Attwood D. Modelling the cure of a commercial epoxy resin for applications in resin transfer moulding. *Polym Int* **41,** 183-191 (1996).

[13] Msallem A. *Caractérisation thermique et mécanique d'un matériau composite aéronautique pendant le procédé d'élaboration - Contribution à l'estimation des contraintes résiduelles*. PhD Thesis, Ecole Centrale de Nantes (2008).

[14] Prasatya P., McKenna G.B., Simon S.L. A viscoelastic model for predicting isotropic residual stresses in thermosetting materials: Effects of processing parameters. *J Compos Mater* **35,** 826-848 (2001).

[15] Kim Y.K., White S.R. Stress relaxation behavior of 3501-6 epoxy resin during cure. *Polym Eng Sci* **36,** 2852-2862 (1996).

[16] Hirsekorn M., Petitjean F., Deramecourt A. A continuous threshold model for the visco-elasto-plastic behavior of PET based multi-layer polymeric films. *Mech Time-Depend Mater* **14,** 25-45 (2010).

[17] Hirsekorn M., Grail G., Carrere N. *Multi-scale modeling of the effect of damage in woven fiber reinforced composites* in Proceedings of *ECCM14*, Budapest, Hungary (2010).

[18] Foreman J.P., Porter D., Behzadi S., Jones F.R. A model for the prediction of structure-property relations in cross-linked polymers. *Polymer* **49,** 5588-5595 (2008).